Journal of Engineering Science and Technology
Vol. 18, No. 1 (2023) 706 - 720

ANALYSIS OF ADSORPTION ISOTHERM CHARACTERISTICS FOR REMOVING CURCUMIN DYES FROM AQUEOUS SOLUTIONS USING AVOCADO SEED WASTE CARBON MICROPARTICLES ACCOMPANIED BY COMPUTATIONAL CALCULATIONS

ASEP BAYU DANI NANDIYANTO*,
DWI NOVIA AL HUSAENI, RISTI RAGADHITA, MELI FIANDINI,
DWI FITRIA AL HUSAENI, RINA MARYANTI

Universitas Pendidikan Indonesia, Jl. Dr. Setiabudi No. 229 Bandung, Indonesia
*Corresponding Author: nandiyanto@upi.edu

Abstract

This study aims to analyse and find isotherm adsorption to remove dye when using calcium carbonate fabricated from avocado seed waste with a computational model of calculation. To obtain calcium carbonate, the avocado seed waste carbonization process was carried out at a temperature of 230˚C for 3 hours and using milling. A batch-reactor technique was used to investigate the adsorption isotherm model. Curcumin was used as a dye model which was adsorbed under constant pressure, pH, and temperature conditions. The adsorption results then used ten adsorption isotherm models, including Langmuir, Freundlich, Temkin, Dubinin-Radushkevich, Fowler-Guggenheim, Hill-DeBoer, Jovanovic, Harkin-Jura, Flory-Huggins, and Halsey. In addition, the calcium carbonate characterization process was also carried out using an optical microscope, sieve test, and Fourier transforms infrared instrument. The results of this study indicate that there are two suitable models to represent the adsorption method, namely Langmuir and Hill-DeBoer. The model was taken based on research data with a regression value/correlation coefficient (R^2) of 0.95. In general, it can be concluded that the adsorption process in this study is attractive, profitable, and spontaneous. The adsorption process is a cooperative monolayer and multilayer. The types of interactions that occur are chemical and physical adsorption. This research shows that avocado seed waste carbon microparticles can be used as an adsorbent to treat coloured waste.

Keywords: Adsorption, Adsorption isotherm, Avocado seed waste, Calcium carbonate.

1. Introduction

Water is one of the basic human needs, both for daily needs (such as drinking and cooking) and agricultural needs [1]. The supply of clean water is getting less and less with the increasing number of textile industries that are established. Many of them dispose of textile dyeing waste carelessly. Though it can endanger the ecosystem of life in the air and can also interfere with human health. Therefore, an effort is needed to be able to remove the dye in the water. One way to purify or clean water from dyes is to use an adsorption technique. According to Azmiyawati [2] adsorption itself is a process of accumulation of the number of molecules, either compounds, ions, or atoms that occur at the boundary between the four phases, namely:

(i) Interaction between the liquid phase and liquid phase.

(ii) Interaction between gas phase and liquid phase.

(iii) Interaction between gas phase and solid phase.

(iv) Interaction between the liquid phase and solid phase.

Adsorption is divided into two parts, namely chemical and physical adsorption. In physical adsorption, the bond strength at each adsorbed molecules are very weak, while in chemical adsorption the bond plays a very important role and is the result of electron transfer in the reaction between the adsorbent and adsorbent. Before the stipulation of this adsorption technique, several techniques could be used to treat dye waste in the aquatic environment, but these techniques were not effective because the dye molecules were dominantly neutral or negatively charged in industrial water. One such technique is the advanced oxidation technique [3].

The use of adsorption techniques can save energy, time, and costs. According to Waluyo et al. [4], the adsorption technique is considered an economical and effective method because it is relatively inexpensive, can be regenerated, and is relatively simple to work on. Several agricultural products are prospective to be used as adsorbents, such as activated charcoal, breadfruit, bagasse, noni fruit, and salak seeds. These materials have been studied by previous researchers. Table 1 shows some previous studies on adsorption.

The difference between our current research and the previous one lies in the type of agricultural material used as an adsorbent. In this study, we used avocado seeds as an adsorbent in the adsorption process. Avocado seeds have several contents in them, such as water content (12.67%), ash content (2.75%), and mineral content (0.54%). Avocado seeds also have a fairly high starch content, which is about 23% with relatively less cellulose content compared to starch content. This causes avocado seed waste to have the potential to be used as an adsorbent material [3].

The purpose of this study was to analyse the characteristics and evaluate the adsorption isotherm on dye removal in an aqueous solution using calcium carbonate fabricated from avocado seed waste. In addition to the use of agricultural materials that are different from previous studies, another difference in this study is that in this study we analysed the isotherm adsorption of calcium particles from avocado seed waste. This study will aid in understanding the phenomena that occur during the adsorption process and will be useful for future applications, particularly when using carbon from organic waste as a catalyst and adsorbent.

Table 1. Several previous studies regarding the use of agricultural materials in the adsorption process.

Type of agricultural material used as adsorbent	Results	Ref.
Palm oil	Oil palm has a large surface area, is easy to obtain, and is relatively inexpensive when compared to other adsorbents.	[5]
Breadfruit	Breadfruit contains cellulose with a level of 17.59% so it can be used as an adsorbent.	[6]
Noni Fruit	Noni juice can help improve the quality of used cooking oil so that it can be used as a medium for frying again.	[7]
Sugarcane Dregs	The use of ICP-MS is highly recommended to reduce iron content in water.	[8]
Salak Seeds	Salak seed bio sorbent has the ability to adsorb dyes and heavy metal chromium.	[9]
Rice Husk	The prepared agglomeration carbon particles, having a size of about 800 nm, are efficient to use as adsorbents.	[10]
Coconut Coir	With an adsorption constant of 0.01-gram mg^{-1} $minute^{-1}$ and a pseudo-second-order reaction kinetics model, adsorption with coconut coir adsorbent followed a pseudo-second-order reaction kinetics model.	[11]
Reed Plants	Under alkaline conditions of pH 9, cellulose adsorbent from the reed plant can adsorb methylene blue dye with a second-order kinetics rate and tends to be multilayer interaction or the concept of Freundlich adsorption isotherm.	[12]
Pumpkin	Adsorption on the surface of pumpkin carbon microparticles occurred as a monolayer with physical phenomena, according to the results.	[13]
Pineapple Peel Waste	The results of this study indicate that the adsorption profile with carbon multiparticle from pineapple peel waste as an adsorbent is following the Freundlich model. Multilayer adsorption process on heterogeneous surfaces and interactions between adsorbate molecules.	[14]
Banana Stem Waste	The adsorption process is included in the monolayer with the type of physical adsorption interaction. Banana stem waste carbon has the potential to be used as an adsorbent	[15]
Rice Straw Waste	This study shows that the use of rice straws is effective for making porous carbon particles and the change in porosity has a direct impact on the product's ability to adsorb molecules.	[16]
Silika Particle from Rice Husk	Silica particles from rice husk proved to be effective in the adsorption of curcumin molecules.	[17]

Type of agricultural material used as adsorbent	Results	Ref.
	The adsorption model that is suitable for this research is the Freundlich isotherm model.	
Soursop Peel Waste	Particle size effects in predicting the adsorption process. The type of interaction that occurs in the adsorption process using soursop peel waste material occurs on the multilayer surface and the adsorbent-adsorbate interaction.	[18]
Red Dragon Fruit Peel Waste	The Dubinin-Radushkevich isotherm model is the most appropriate adsorption isotherm model with Red Dragon Fruit Peel Waste as the adsorbent.	[19]
Calcium Carbonate from Barred Fish (Scomberomorus spp.) Bone	The Dubinin-Radushkevich isotherm model is the most appropriate adsorption isotherm model. The findings reveal that the multilayer adsorption process occurs for all micrometre sizes and that the process involves physical interactions between the adsorbate and the adsorbent surface.	[20]

2. Isotherm Adsorption Model Used in This Study

Adsorption isotherm models such as Langmuir, Freundlich, Temkin, Dubinin-Radushkevich, Fowler-Guggenheim, Hill-Deboer, Jovanovic, Harkin-Jura, Flory-Huggins, and Halsey were used to study the phenomena during the adsorption process [21]. In the adsorption process in general 3 phenomena may occur, namely monolayer, multilayer, and cooperative. Figure 1 shows an illustration of the three phenomena.

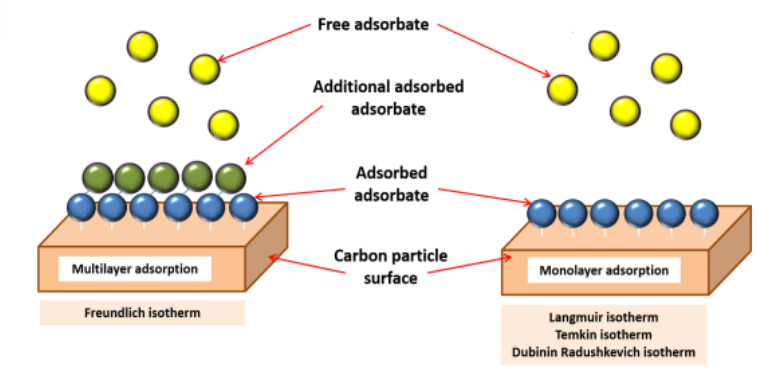

Fig. 1. Illustration of monolayer, multilayer, and cooperative (adopted from reference [14]).

2.1. Langmuir isotherm

The Langmuir isotherm is based on the adsorption process that takes place on a homogenous surface to generate a monolayer. Because no adsorbate transmigrates, the monolayer assumes that the molecules adsorbed during the adsorption process do not interact with one other and hence have the same surface energy. The development of monolayer sites on this adsorbent's surface hinders subsequent

adsorption activities. Equations (1) and (2) can be used to predict the Langmuir isotherm equation [21].

$$\frac{1}{Q_e} = \frac{1}{Q_{max} K_L} \frac{1}{C_e} + \frac{1}{Q_{max}} \quad (1)$$

$$R_L = \frac{1}{1 + K_L C_e} \quad (2)$$

where K_L is the Langmuir adsorption constant, Q_{max} is the adsorption capacity of the monolayer (mg/g), and R_L is the separation factor. Table 2 explains about R_L parameter.

Table 2. The meaning of the R_L parameter.

Condition of the R_L	Description
$R_L > 1$	Adsorption is unfavourable because desorption occurs.
$R_L = 1$	Adsorption procedure that is linear and does not depend on concentration.
$R_L = 0$	Because the adsorbate cannot diffuse, the adsorption process is irreversible (usually occurs in chemisorption)
$0 < R_L < 1$	Adsorption is advantageous since no desorption occurs.

2.2. Freundlich isotherm

Freundlich isotherm is based on the adsorption process that occurs on heterogeneous surfaces that form multilayers. Multilayer adsorption allows interactions between adsorbed molecules, so this model implies that the energy is not the same at each surface site. Freundlich's isotherm model can be expressed by Eq. (3) [21].

$$\log Q_e = log k_f + \frac{1}{n} \log C_e \quad (3)$$

where k_f is the Freundlich constant that estimates the adsorption capacity, C_e is the adsorbate concentration at equilibrium (mg/L), n is the degree of non-linearity, and $1/n$ assumes the adsorption strength. Table 3 explains about n and $\frac{1}{n}$ parameters condition and description.

Table 3. The meaning of the n and $\frac{1}{n}$ parameters.

Condition of n and $\frac{1}{n}$	Description
$n < 1$	Characteristics of the adsorption and chemisorption processes.
$n = 1$	Characteristic of a linear adsorption process in which there is a concentration-independent partition between two phases.
$n > 1$	Characteristics of the physisorption process concerning adsorption.
$\frac{1}{n} < 1$	Normal adsorption process characteristics.
$\frac{1}{n} > 1$	Characteristics of the cooperative adsorption process.
$1 < \frac{1}{n} < 0$	Because there is no desorption process, this is a beneficial adsorption process.
$0 < \frac{1}{n} < 1$	Adsorption process on heterogeneous surfaces ($\frac{1}{n}$ value close to 0 suggests that the adsorbent surface is becoming increasingly heterogeneous).

2.3. Temkin isotherm

Indirect adsorbate interaction when the adsorbate concentration is described by the Temkin isotherm. The concentration of adsorbate used is very low [21]. Equation (4) is used to calculate the adsorption heat for all molecules in the multilayer.

$$q_e = \beta_T(lnC_e) + (\beta_T lnA_T) \quad (4)$$

where A_T is the equilibrium constant of the Temkin isotherm model, and β_T is the Temkin isotherm. Table 4 explains about β_T parameter.

Table 4. The meaning of the β_T parameter.

Condition of the β_T parameter	Description
β_T < 8 kJ/mol	Physical adsorption
β_T > 8 kJ/mol	Chemical adsorption

2.4. Dubinin-Radushkevich isotherm

The Dubinin-Raduskevich isotherm is based on the assumption that adsorption takes place on heterogeneous surfaces [21]. Equation (5) depicts the Dubinin-Radushkevich model's adsorption equation.

$$lnq_e = lnq_s - \beta\varepsilon^2 \quad (5)$$

where q_s is the theoretical saturation capacity (mg/g) and ε is the Polanyi potential associated with equilibrium conditions.

The Polanyi potential and the calculation of the adsorption energy are expressed by Eqs. (6) and (7).

$$\varepsilon = RT \ln\left[1 + \frac{1}{C_e}\right] \quad (6)$$

$$E = \frac{1}{\sqrt{2\beta}} \quad (7)$$

where E is the adsorption energy which has described that shown in Table 5.

Table 5. The meaning of the *E* parameter.

Condition of *E* parameter	Description
***E* < 8 kJ/mol**	Physical adsorption
***E* > 8 kJ/mol**	Chemical adsorption

2.5. Flory-Huggins isotherm

The Flory-Huggins isotherm considers the adsorbate's surface coverage on the adsorbent and assumes that the adsorption process occurs spontaneously [21]. The Flory-Huggins isotherm is represented by Eq. (8).

$$log\frac{\theta}{C_e} = logK_{FH} + n\log(1-\theta) \quad (8)$$

where θ is the constant, following $\theta = (1 - \frac{C_e}{C_o})$ which indicates the degree of surface coverage, n_{FH} is the amount of adsorbate occupying the adsorption site, and K_{FH} is the Flory-Huggins isotherm constant.

To compute the Gibbs free energy (ΔG°) of spontaneous adsorption, the value of ΔG° can be estimated from the equilibrium constant (K_{FH}), as stated in Eq. (9).

$$\Delta G° = -RT\ln K_{FH} \quad (9)$$

The fact that ΔG° is negative suggests that the adsorption process is spontaneous and temperature-dependent.

2.6. Fowler-Guggenheim isotherm

The Fowler-Guggenheim isotherm illustrates how adsorbed molecules interact with one another [21]. Equation (10) expresses the Fowler-Guggenheim isotherm equation.

$$K_{FG} C_e = \frac{\theta}{1-\theta} \exp\left(\frac{2.\theta.W}{RT}\right) \quad (10)$$

where K_{FG} is the Fowler-Guggenheim equilibrium constant (L/mg), and W is the interaction energy between the adsorbed molecules (kJ/mol). Table 6 outlines the significance of the W parameter.

Table 6. The meaning of the *W* parameter.

Condition of the *W* parameter	Description
***W* > 0 kJ/mol**	The reaction is exothermic due to the attractive force between the adsorbed molecules.
***W* < 0 kJ/mol**	The reaction is endothermic due to the repulsion between the adsorbed molecules.
***W* = 0 kJ /mol**	No contact between the molecules has been adsorbed.

2.7. Hill-de Boer isotherm

Mobile adsorption and the presence of bilateral interactions between the adsorbed molecules are described by the Hill-de Boer isotherm [21]. Equation (11) expresses the Hill-de Boer isotherm equation.

$$K_1 . C_e = \frac{\theta}{1-\theta} \exp\left(\frac{\theta}{1-\theta} - \frac{K_2\theta}{RT}\right) \quad (11)$$

where K_1 is the Hill-de Boer constant (L/mg), and K_2 is the energetic constant of the adsorbed molecular interaction. Table 7 shows the meaning of K_2 parameter.

Table 7. The meaning of the K_2 parameter.

Condition of the K_2 parameter	Description
K_2 > 0 kJ/mol	The reaction is exothermic due to the attractive force between the adsorbed molecules.
K_2 < 0 kJ/mol	The reaction is endothermic due to the repulsion between the adsorbed molecules.
K_2 = 0 kJ/mol	No contact between the molecules has been adsorbed.

2.8. Jovanovic isotherm

The Jovanovic isotherm is based on the Langmuir model's phenomena, but it does not accept a mechanical connection between the adsorbate and adsorbent [21]. Equation (12) depicts the linear equation of the Jovanovic isotherm.

$$\ln Q_e = \ln Q_{max} - K_j C_e \quad (12)$$

where Q_e is the amount of adsorbate in the adsorbent at equilibrium (mg/g), K_J is the Jovanovic constant, and Q_{max} is the maximum absorption of the adsorbate.

2.9. Harkin-Jura isotherm

The Harkin-Jura isotherm assesses adsorption on a heterogeneous surface where adsorption happens by producing a multilayer [21]. Equation (13) represents the equation of this model.

$$\frac{1}{q_e^2} = \frac{B_{HJ}}{A_{HJ}} - \left(\frac{1}{A}\right) log C_e \tag{13}$$

where B_{HJ} is the specific surface area of the adsorbent and A_{HJ} is the Harkin-Jura isotherm constant.

2.10. Halsey isotherm

The Halsey isotherm is used to analyse adsorption with multilayer properties [21]. Equation (14) depicts the Halsey isotherm equation.

$$Q_e = \frac{1}{n_H} lnK_H - \left(\frac{1}{n_H}\right) lnC_e \tag{14}$$

where K_H is the Halsey's isotherm constant and N is the Halsey's isotherm constants.

Table 8 details the curves of the data fitting result and the computation of each adsorption isotherm parameter.

Table 8. Adsorption isotherms fitting data, calculation, and their parameter.

Isotherm Model	Linear Equation	Plotting		Parameters		
		x	y	Intercept	Slope	Others
Langmuir	$\frac{1}{Q_e} = \frac{1}{Q_{max} K_l} \frac{1}{C_e} + \frac{1}{Q_{max}}$	$\frac{1}{C_e}$	$\frac{1}{Q_e}$	$\frac{1}{Q_{max}}$	-	$K_L = \frac{1}{Q_{max} \times slope}$
Freundlich	$\log Q_e = log k_f + \frac{1}{n} \log C_e$	lnC_e	lnQ_e	lnK_F	$\frac{1}{n}$	-
Temkin	$q_e = \beta_T (lnC_e) + (\beta_T lnA_T)$	lnC_e	Q_e	$B_T lnA_T$	B	$B_T = \frac{RT}{B}$
Dubinin-Radushkevich	$lnq_e = lnq_s - \beta\varepsilon^2$	ε^2	lnQ_e	-	$\beta = K_{DR}$	$E = \frac{1}{\sqrt{2 \times K_{DR}}}$
Flory Huggins	$log \frac{\theta}{C_e} = log K_{FH} + n\log (1 - \theta)$	$\log\left(\frac{}{}\right.$	$log(1-\theta)$	k_{FH}	n_{FH}	$\Delta G^o = RTln(k_{FH})$ $\theta = 1 - (\frac{C_e}{C_0})$
Fowler-Guggenheim	$ln\left(\frac{C_e(1-\theta)}{\theta}\right) - \frac{\theta}{1-\theta} = -lnK_{FG} + \frac{2W\theta}{RT}$	θ	$ln\left[\frac{C_e(1-\theta)}{\theta}\right]$	$-lnK_{FG}$	W	$\alpha\ (slope) = \frac{2W\theta}{RT}$ $\theta = 1 - (\frac{C_e}{C_0})$
Hill-Deboer	$ln\left[\frac{C_e(1-\theta)}{\theta}\right] - \frac{\theta}{1-\theta} = -lnK_1 - \frac{K_2\theta}{RT}$	θ	$ln\left[\frac{C_e(1-\theta)}{\theta}\right] - \frac{\theta}{1-\theta}$	$-lnk_1$	-	$\alpha\ (slope) = \frac{k_2\theta}{RT}$ $\theta = 1 - (\frac{C_e}{C_0})$
Jovanovic	$lnQ_e = lnQ_{max} - K_j C_e$	C_e	lnQ_e	lnq_{max}	K_J	-
Harkin-Jura	$\frac{1}{q_e^2} = \frac{B_{HJ}}{A_{HJ}} - \left(\frac{1}{A}\right) log C_e$	$logC_e$	$\frac{1}{q_e^2}$	$\frac{B_H}{A_H}$	$A_H = \frac{1}{Slope}$	-
Halsey	$Q_e = \frac{1}{n_H} lnK_H - \left(\frac{1}{n_H}\right) lnC_e$	lnC_e	lnQ_e	$\frac{1}{n} lnK_H$	$\frac{1}{n}$	-

Furthermore, the unit mass of the adsorbent at equilibrium (*Qe*) is calculated using Eq. (16).

$$Q_e = \frac{C_o - C_e}{m} \times V \quad (15)$$

where C_o is the initial concentration (mg/L), C_e is the equilibrium concentration (mg/L), m is the mass of the adsorbent (g), and V is the volume of the adsorbate solution (L).

3. Materials and Method

3.1. Materials

In this study, distilled water and avocado seed waste were used as material (purchased from a traditional market in Bandung, Indonesia), and curcumin (obtained utilizing the turmeric extraction process). Details of the turmeric extraction process are reported in the literature [22].

3.2. Preparation of calcium carbonate particles from avocado seeds

Avocado seed samples were separated from the flesh. Then wash it clean. After that, it was carbonized using an oven at 230˚C for 3 hours. To obtain durian seed particles with a homogeneous size, the durian seed sample will be ground using a saw-milling tool for ± 2 minutes. After completion, the particles were filtered using a tool called a sieve-test (PT Rumah Publication Indonesia) with sieve-mesh hole sizes of 500, 250, 100, 74, and 60 m to obtain specific sizes.

3.3. Particles characterization

The particle size and morphology of the raw material were investigated with a digital microscope (calcium carbonate from chicken bone waste). Chemical characterization of elemental structure products was carried out using Fourier transform infrared (FTIR, FTIR-6600, Jasco Corp., Japan).

3.4. Batch adsorption experimental

In a beaker glass with a volume of 140 mL, calcium carbonate particles (as adsorbent) were added to as much as 0.05 g of curcumin solution with specified concentrations of 100, 80, 60, 40, and 20 ppm (batch experiment). At ambient circumstances with a constant pH, the adsorption test was performed by mixing the curcumin-carbon solution at 1000 rpm for 120 minutes (approximately 7). An aliquot of the combined solution was collected and filtered using a nylon membrane syringe filter with a pore size of 0.22 um to assess adsorption. The concentration of the solution following the adsorption process was then determined using a Visible Spectroscopy (Model 7205; JENWAY; Cole-Parner; US) with a maximum wavelength of 280 to 500 nm. The results of the adsorption were plotted and normalized. Beer's Law was used to determine the concentration of curcumin by calculating the maximal absorption peak. The results are plotted and compared with ten models of isotherms, there are (i) Langmuir; (ii) Freundlich; (iii) Temkin; (iv) Dubinin-Radushkevich; (v) Fowler-Guggenheim; (vi) Hill-Deboer; (vii) Jovanovic; (viii) Harkin-Jura; (ix) Flory-Huggins; (x) Halsey adsorption isotherm models.

4. Results and Discussion

Figure 2(a) shows a digital microscope image of the carbon particles of durian seed waste. If observed using ferret analysis, it will be found that the carbon particles have sizes in the range of 320 – 1000 m. Figure 2(a) also shows that the calcium carbonate particles have an inhomogeneous size. While Fig. 2(b) shows the distribution results where most of the particle sizes of avocado seed waste are. Carbon particles mostly have several sizes with calcium carbonate particles having sizes in the range of 100 and 500 um. The average particle size of calcium carbonate is 274.48 um with a standard deviation of 18.89 um.

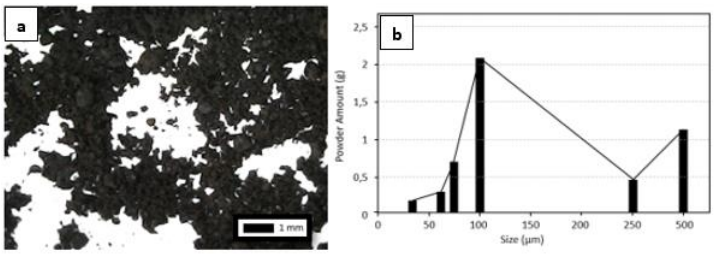

Fig. 2. Photograph image of carbon particles (a) and their particle size distribution (b).

Figure 3 shows the results of fitting the adsorption process with 10 adsorption isotherm models. Based on the results of the data fitting process with the adsorption isotherm model, 2 models are suitable to describe the adsorption process in this study, namely the Langmuir model and the Hill-Deboer model. The selection of the appropriate model is based on the value of the correlation coefficient, which is 0.95. More detailed data will be presented in Table 9.

Figure 3(a) shows the results of the analysis of the Langmuir isotherm model. The analysis process is carried out based on Eqs. (1) and (2). The adsorption data on the Langmuir isotherm model shows the value of R^2 = 0.974 with the maximum adsorption capacity parameter value (Qmax) being 1.785 mg/g (see Table 9). The value of the R_L parameter on the Langmuir isotherm (see Table 1) shows that its value is in the range $R_L > 0$ and $R_L < 1$. Figure 3(b) shows the results of fitting adsorption data based on Eq. (3). The Freundlich model shows the value of R^2 = 0.948. The value of parameter n on the Freundlich isotherm is 0.390 and the value of parameter 1/*n* is 2.564 (see Table 9). Parameter values that indicate $n > 1$ and $1/n > 1$ inform that the adsorption process occurs cooperatively.

Figure 3(c) was analysed using Eq. (4). The Temkin model assumes that all molecules on the surface of the adsorbent have a linearly decreasing heat of adsorption due to uniform energy distribution. The Temkin isotherm model has a value of R^2 = 0.691 and a parameter value of $\beta_T < 8$ kJ/mol (see Table 9). Figure 3(d) shows the plotting results based on the linear equation, Equation (5), of Dubinin-Raduskevich. The Dubinin-Radushkevich isotherm has a value of R^2 = 0.910 and the value of the parameter *E* isotherm is 0.467 (see Table 9). E value < 8 kJ/mol which indicates that the adsorption process is going physically (physisorption) [21].

Figure 3(e) shows the results of plotting analysis build upon the Fowler Guggenheim isotherm using Eq. (8). The R^2 value of this equation is 0.9463 and the value of the W parameter is 1152.66 kJ/mol (see Table 9). Figure 3(f) is the resulting curve of plotting data on the Hill-Deboer isotherm, Eq. (9). The Hill-Deboer isotherm has a value of $R^2 = 0.954$ with a K2 parameter value of -1122.686 (see Table 9). Based on the value of the K2 parameter (K2 < 0 kJ/mol), the adsorption process occurs with interactions between molecules that repel each other, and the process is endothermic [21].

Figure 3(g) is the result of plotting data based on the Jovanovic isotherm model using Eq. (10). Based on the results of plotting the Jovanovic isotherm, the adsorbent capacity (Qmax) is 1.363 (see Table 9). The Qmax value indicates that the Qmax value is relatively small, indicating that the adsorbent has a weak adsorption capacity [21].

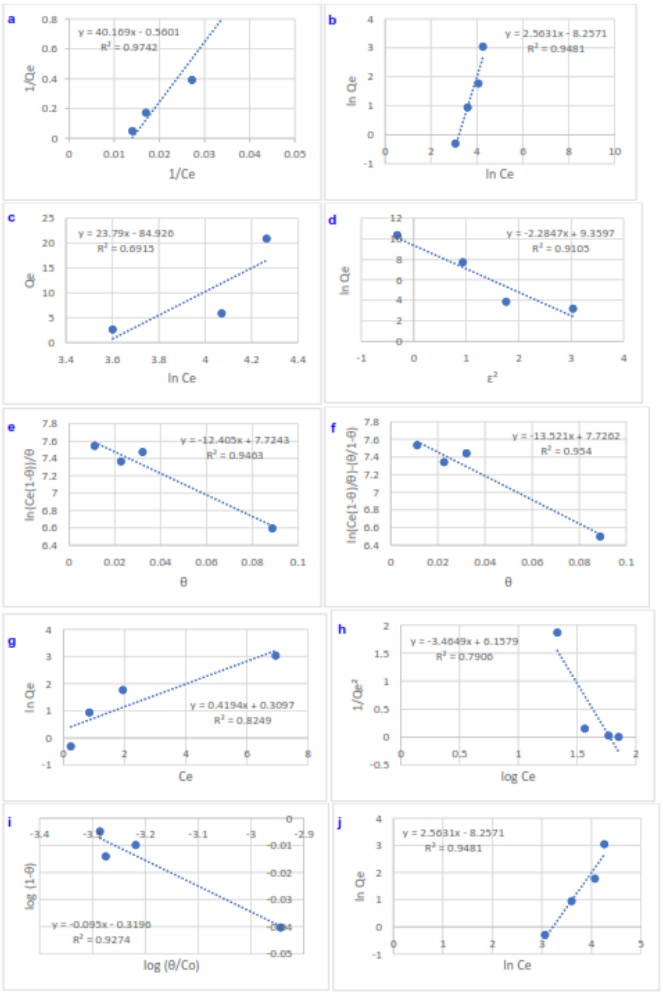

Fig. 3. Data fitting with isotherm models Langmuir (a), Freundlich (b), Temkin (c), Dubinin-Radushkevich (d), Fowler-Guggenheim (e), Hill-Deboer (f), Jovanovic (g), Harkin -Jura (h), Flory-Huggins (i), and Halsey (j)

Figure 3(h) is the Harkin-Jura adsorption model whose adsorption parameters are shown by Eq. (11). The results of the curve analysis of the Harkin-Jura isotherm show that R^2 is 0.790 (see Table 9). Harkin-Jura isotherm parameters identified are *AHJ* and *BHJ* parameters with values of 0.288 and 1.773, respectively (see Table 9) [21].

Figure 3(i) shows plotting analysis based on Flory-Huggins (Eq. (11)). The correlation coefficient value of this model is R^2 = 0.9274 (see Table 9). The existence of interactions between free molecules and adsorbed molecules on the surface of the adsorbent was investigated from the parameter value of n_{FH}. The interaction occurs because the free molecule attaches and interacts with the adsorbed molecule. The value of the Gibbs free energy is also informed by this model. The Gibbs free energy parameter has a negative value which indicates that the adsorption process is spontaneous [21]. Figure 3(j) is the result of plotting the data against the Halsey isotherm using Eq. (14). The Halsey isotherm shows the value of R^2 = 0.948 with the Halsey isotherm constants for *KH* and *n* are -5.538 and 0.390, respectively (see Table 9) [21].

Table 9. Detailed data of adsorption isotherm parameters.

Model	Parameters	Value	Notes
Langmuir	R^2	0.974	Monolayer adsorbent process ($R^2 < 0.90$)
	Q_{max} (mg/g)	1.785	Maximum capacity adsorption
	K_L (L/mg)	0.013	Small worth The Langmuir constant indicates that there is little interaction between the adsorbate and the adsorbent.
	R_L	0.793	Favourable adsorption (0 < RL <1)
Freundlich	R^2	0.948	Multilayer existence on the surface of adsorbent ($R^2 > 0.90$)
	n	0.390	Physisorption process ($n > 1$)
	$1/n$	2.564	Cooperative adsorption process ($1/n > 1$)
	K_f (mg/g)	12.975	Adsorption capacity of adsorbent
Temkin	R^2	0.691	Uniform distribution adsorbate in the adsorbent surface (R2 > 0.90)
	A_T (L/g)	2.419	Temkin equilibrium binding constant
	β_T (J/mol)	95.406	Physical adsorption ($\beta_T < 8$ kJ/mol)
Dubinin-Radushkevich	R^2	0.910	The adsorbent surface contains micropores ($R^2 > 0.90$)
	β (mol^2/kJ^2)	2.284	Dubinin-Radushkevich isotherm constant
	E (kJ/mol)	0.467	Physical adsorption ($E < 8$ kJ/mol)
Fowler-Guggenheim	R^2	0.946	Multilayer existence on the surface of adsorbent ($R^2 > 0.90$)
	W (kJ/mol)	1152.662	Attractive interactions that occur between adsorbed molecules (W < 0 kJ/mol)
	K_{FG} (L/mg)	441×10^{-6}	Fowler-Guggenheim isotherm constant
Hill-Deboer	R^2	0.954	Multilayer existence on the surface of adsorbent ($R^2 > 0.90$)
	K_1 (L/mg)	$44\text{x}10^{-6}$	Hill-Deboer isotherm constant
	K_2 (kJ/mol)	-1122.686	Repulsive interactions that occur between adsorbed molecules ($K_2 < 0$ kJ/mol)
Jovanovic	R^2	0.824	Multilayer existence on the surface of adsorbent ($R^2 > 0.90$)
	K_J (L/mg)	0.338	Jovanovic isotherm constant
	Q_{max} (mg/g)	1.363	Maximum uptake of adsorbate
Harkin-Jura	R^2	0.790	Multilayer existence on the surface of adsorbent ($R^2 > 0.90$)

	A_{HJ}	0.288	Harkin-Jura isotherm constant
	B_{HJ}	1.773	Related to the surface area of the adsorbent
Flory-Huggins	R^2	0.927	Multilayer existence on the surface of adsorbent ($R^2 > 0.90$)
	n_{FH}	-0.095	The adsorbate occupies more than one active adsorbent zone ($n_{FH} < 1$)
	K_{FH} (L/mg)	0.479	Flory-Huggins isotherm constant
	$\Delta G°$	-0.736	Spontaneously adsorption ($\Delta G° < 0$)
Halsey	R^2	0.948	Multilayer existence on the surface of adsorbent ($R^2 > 0.90$)
	n	0.390	Halsey isotherm constant
	K_H	-5.538	Halsey isotherm constant

As previously explained, adsorption isotherms are used to find an adsorption model that can clearly describe the adsorption process. The value of the correlation coefficient (R^2) can be used as a value to determine the suitability of the adsorption isotherm model. The isotherm model is said to be suitable if the value of R^2 is close to the value of 1. A suitable isotherm model can be ordered based on the value of R^2 as follows:

(i) Langmuir (R^2 = 0.974)
(ii) Hill-Deboer (R^2 = 0.954)
(iii) Freundlich (R^2 = 0. 948)
(iv) Halsey (R^2 = 0.948)
(v) Fowler-Guggenheim (R^2 = 0.946)
(vi) Flory-Huggins (R^2 = 0.927)
(vii) Dubinin-Radushkevich (R^2 = 0.910)
(viii) Jovanovic (R^2 = 0.824)
(ix) Harkin-Jura (R^2 = 0.790)
(x) Temkin (R^2 = 0.691)

The adsorption process followed monolayer adsorption because it had the best match with the Langmuir isotherm with a relativity coefficient value (R^2) = 0.974, according to the results of the adsorption process analysis on the most suited adsorption isotherm model. Other models with good correlation coefficients (R^2 > 0.90) after being confirmed by the total isotherm value include Hill-Deboer, Freundlich, Halsey, Fowler-Guggenheim, Flory-Huggins, Dubinin-Radushkevich, adsorption method for multilayer adsorption. Although multilayer adsorption occurs, the chemical connection between adsorbate and adsorbate is weak, resulting in physisorption. Freundlich, Temkin, and Dubinin-isotherm Radushkevich's model validated this physisorption interaction mechanism. In addition, overall the adsorption process was cooperative (confirmed by the Freundlich isotherm) and favourable (confirmed by the Freundlich isotherm). Based on the Flory-Huggins isotherm, the adsorption process does spontaneously. This study can bring a new reference for the adsorption process of particles and can add and complete our list of adsorption characteristics of some materials [13-23].

5. Conclusion

This study aims to analyse the characteristics and evaluate the adsorption isotherm on dye removal in an aqueous solution using calcium carbonate fabricated from avocado seed waste. The process of carbonization of durian seed waste is carried out to obtain calcium carbonate. The Batch technique was used to investigate the

adsorption isotherm model. Curcumin was used as a colour model. The results of this study indicate that several models are suitable to represent adsorption equilibrium where the correlation coefficient value is close to 1, namely Langmuir ($R^2 = 0.9742$), and Hill-Deboer ($R^2 = 0.954$). Avocado seeds are used because they have a fairly high starch content, with a relatively lower cellulose content. In this study, it was also found that alternative calcium carbonate materials derived from avocado seeds can be used as an adsorbent to treat coloured waste. Calcium carbonate particles can absorb curcumin molecules as a model of the adsorbate.

References

1. Hartono, B.; and Purwanto, P. (2015). Perancangan pompa air tenaga surya guna memindahkan air bersih ke tangki penampung. *Sintek Jurnal: Jurnal Ilmiah Teknik Mesin*, 9(1), 28-33.
2. Azmiyawati, C. (2006). Kajian kinetika adsorpsi Mg (II) pada silika gel termodifikasi gugus sulfonat. *Jurnal Kimia Sains dan Aplikasi*, 9(2), 35-39.
3. Hamzezadeh, A.; Rashtbari, Y.; Afshin, S.; Morovati, M.; and Vosoughi, M. (2022). Application of low-cost material for adsorption of dye from aqueous solution. *International Journal of Environmental Analytical Chemistry*, 102(1), 254-269.
4. Waluyo, U.; Ramadhani, A.; Suryadinata, A.; and Cundari, L. (2020). penjernihan minyak goreng bekas menggunakan berbagai jenis adsorben alami. *Jurnal Teknik Kimia*, 26(2), 70-79.
5. Adam, D.H. (2017). Kemampuan tandan kosong kelapa sawit sebagai adsorben untuk meregenerasi minyak jelantah. *Jurnal Eduscience (Jes)*, 4(1), 8-11.
6. Suartini, N.; Jamaluddin, J.; and Ihwan, I. (2018). Pemanfaatan arang aktif kulit buah sukun (Artocarpus altilis (Parkinson) Fosberg) sebagai adsorben dalam perbaikan mutu minyak jelantah. *KOVALEN: Jurnal Riset Kimia*, 4(2), 152-165.
7. Juliana, I.N.; Gonggo, S.T.; and Said, I. (2015). Pemanfaatan buah mengkudu (*Morinda citrifolia L*.) sebagai adsorben untuk meningkatkan mutu minyak jelantah. *Jurnal Akademika Kimia*, 4(4), 181-188.
8. Imani, A.; Sukwika, T.; and Febrina, L. (2021). Karbon aktif ampas tebu sebagai adsorben penurun kadar besi dan mangan limbah air asam tambang. *Jurnal Teknologi*, 13(1), 33-42.
9. Hanifah, H.N.; Hadisoebroto, G.; Apriani, R.; and Apriani, M. (2020). Efektivitas kulit salak dan biji salak (*Salacca zalacca*) sebagai bioadsorben logam pb dari limbah cair laboratorium farmasi. *Jurnal Sabdariffarma*, 2(2), 13-20.
10. Fiandini, M.; Ragadhita, R.; Nandiyanto, A.B.D.; and Nugraha, W.C. (2020). Adsorption characteristics of submicron porous carbon particles prepared from rice husk. *Journal of Engineering Science and Technology*, 15, 022-031.
11. Baunsele, A.B.; and Missa, H. (2020). Kajian kinetika adsorpsi metilen biru menggunakan adsorben sabut kelapa. *Akta Kimia Indonesia*, 5(2), 76-85.
12. Huda, T.; and Yulitaningtyas, T.K. (2018). Kajian adsorpsi methylene blue menggunakan selulosa dari alang-alang. *Indonesian Journal of Chemical Analysis (IJCA)*, 1(01). 9-19.

13. Nandiyanto, A.B.D.; Hofifah, S.N.; Inayah, H.T.; Putri, S.R.; Apriliani, S.S.; Anggraeni, S.; and Rahmat, A. (2021a). Adsorption isotherm of carbon microparticles prepared from pumpkin (*Cucurbita maxima*) seeds for dye removal. *Iraqi Journal of Science*, 1404-1414.
14. Nandiyanto, A.B.D.; Azizah, N.N.; and Rahmadianti, S. (2021b). Isotherm study of banana stem waste adsorbents to reduce the concentration of textile dying waste. *Journal of Engineering Research*, 9, 1-15.
15. Nandiyanto, A.B.D.; Putra, Z.A.; Andika, R.; Bilad, M.R.; Kurniawan, T.; Zulhijah. R.; and Hamidah. I. (2017). Porous activated carbon particles from rice straw waste and their adsorption properties. *Journal of Engineering Science and Technology*, 12(8), 1-11.
16. Ragadhita, R.; Nandiyanto, A.B.D.; Nugrah, W.C.; and Mudzakir, A. (2019). Adsorption isotherm of mesopore-free submicron silica particles from rice husk. *Journal of Engineering Science and Technology*, 14(4), 2052-2062.
17. Nandiyanto, A.B.D.; Girsang, G.C.S.; Maryanti, R.; Ragadhita, R.; Anggraeni, S.; Fauzi, F.M.; Sakinah, P.; Astuti, A.P.; Usdiyana, D.; Fiandi, M.; Dewi, M.W.; and Al-Obaidi, A.S.M. (2020). Isotherm adsorption characteristics of carbon microparticles prepared from pineapple peel waste. *Communications in Science and Technology*, 5(1), 31-39.
18. Nandiyanto, A.B.D.; Arinalhaq, Z.F.; Rahmadianti, S.; Dewi, M.W.; Rizky, Y.P.C.; Maulidina, A.; Anggraeni, S.; Bilad, M.R.; and Yunas, J. (2020). Curcumin adsorption on carbon microparticles: Synthesis from soursop (*Annona muricata L.*) peel waste, adsorption isotherms and thermodynamic and adsorption mechanism. *International Journal of Nanoelectronics and Materials*, 13, 173-192.
19. Nandiyanto, A.B.D.; Maryanti, R.; Fiandini, M.; Ragadhita, R.; Usdiyana, D.; Anggraeni, S.; Arwa, W.R.; and Al-Obaidi, A.S.M. (2020). Synthesis of carbon microparticles from red dragon fruit (*Hylocereus undatus*) peel waste and their adsorption isotherm characteristics. *Molekul*, 15(3), 199-209.
20. Nandiyanto, A.B.D.; Erlangga, T.M.S.; Mufidah, G.; Anggraeni, S.; Bilad, R.; and Yunas, J. (2020). Adsorption isotherm characteristics of calcium carbonate microparticles obtained from barred fish (*Scomberomorus spp*.) bone using two-parameter multilayer adsorption models. *International Journal of Nanoelectronics and Materials*, 13, 45-57.
21. Nandiyanto, A.B.D.; Ragadhita, R.; and Yunas, J. (2020). Adsorption isotherm of densed monoclinic tungsten trioxide nanoparticles. *Sains Malaysiana*, 49(12), 2881-2890.
22. Nandiyanto, A.B.D.; Kim, S.G.; Iskandar, F.; and Okuyama, K. (2009). Synthesis of spherical mesoporous silica nanoparticles with nanometer-size controllable pores and outer diameters. *Microporous and Mesoporous Materials*, 120(3), 447-453.
23. Ragadhita, R.; and Nandiyanto, A.B.D. (2021). How to calculate adsorption isotherms of particles using two-parameter monolayer adsorption models and equations. *Indonesian Journal of Science and Technology*, 6(1), 205-234.